Article

Not peer-reviewed version

# Stochastic Modeling of COVID-19 with the Impact of Vaccination Class, Using Higher-Order Spectral Scheme

Fuad A Awwad * , Sami Ullah Khan , Farman Ullah Khan , Emad A. A Ismail , Taza Gul *

Posted Date: 21 July 2023

doi: 10.20944/preprints202307.1476.v1

Keywords: COVID-19 mathematical model; Vaccination; Stochastic Asymptotic stability; Legendre-Gauss-Lobatto points; Spectral Method

 doi:10.20944/preprints202307.1476.v1



*Article*

# Stochastic Modeling of COVID-19 with the Impact of Vaccination Class, Using Higher-Order Spectral Scheme

**Fuad A. Awwad [1,*], Sami Ullah Khan [2], Farman U Khan [3], Emad A. A. Ismail [1] and Taza Gul [2,*]**

[1] Department of Quantitative analysis, College of Business Administration, King Saud University, P.O. Box 71115, Riyadh 11587, Saudi Arabia

[2] Department of Mathematics, City University of Science and Information Technology Peshawar, KP, 2500, Pakistan

[3] Department of Mathematics, HITEC University, Taxila Cantt, 47080, Pakistan

* Correspondence: fawwad@ksu.edu.sa (F.A.A.); tazagul@cusit.edu.pk (T.G.)

**Abstract:** Coronavirus disease 2019 (COVID-19) is a high contagious respiratory infectious disease that has affected millions of people worldwide. Initially, basic public health measures were implemented to control specially the spread of such virus. However, vaccination has emerged as a highly effective strategy in combating COVID-19 and reducing its transmission. Several effective and safe vaccines have been approved to prevent the inadvertent spread of the disease. In this study, a modeling approach is used to analyze the impact of these vaccines on the dynamics of COVID-19. By applying a higher-order numerical method, the model is solved based on reported cases in Pakistan. A spectral method is employed for the numerical solution, and the model is simulated to assess the effects of vaccination. The Next-generation method is used to calculate the threshold quantity, known as $\mathscr{R}_0$, which indicates the potential for disease transmission. The study also includes a detailed stability analysis, examining the invariance properties of the model solution and discussing equilibrium points and their stability in disease-free and endemic states. Furthermore, the study presents graphical representations of the influence of special parameters on the dynamics of the pandemic.

**Keywords:** COVID-19 mathematical model; vaccination; stochastic asymptotic stability; Legendre-Gauss-Lobatto points; spectral method

## 1. Introduction

The coronavirus infection is a highly contagious viral disease that has effect and spread to almost every country in the world. It is caused by a virus called Severe Acute Respiratory Syndrome coronavirus 2 (SARS-CoV-2) and that was firstly identified in December 2019. In March 2020, the World Health Organization (WHO) declared COVID-19 a pandemic due to its rapid spread and impact on millions of people worldwide [1]. After certain time period COVID-19 has affected more people than previous outbreaks of MERS and SARS. The initial outbreak of COVID-19 cases was detected in Wuhan, China. Many individuals infected with proposed virus may not show any symptoms or only experience mild symptoms. However, those with symptoms typically experience a muscle or joint pain, dry cough, fever and in many active cases, specially shortness of breath which was more painful stage for effected people. COVID-19 poses a significant risk to individuals with pre-existing health conditions such as diabetes, kidney disease, cardiovascular and obesity disease. Most of the people with chronic respiratory diseases are especially vulnerable to severe complications and death from COVID-19. The primary mode of transmission is through direct contact with attenuated objects or surfaces, as well as consumption of respiratory aerosol from infected individuals, whether they show symptoms or not [2].

The COVID-19 pandemic continuously to show mannerism a significant threat to people worldwide, particularly due to the increasing incidence of infection in certain countries. Consequently,

 doi:10.20944/preprints202307.1476.v1



it has become crucial to detect, assess, and understand the exempt feedback to SARS-CoV-2 disease. While diseases like Polio can be controlled by regular vaccination to the children below a certain 5 years of age and most of medicines and antibiotics can help to manage the outbreaks of infection, some infectious diseases such as TB, Cholera, and Malaria still cause fatalities globally [3]. However, recently some effective and safe vaccines have been developed by many countries still rely on non pharmaceutical mediation like social distancing, lock downs, and face masks to contest the infection. Nonetheless, vaccination remains an effective and simple strategy in controlling infectious diseases, as demonstrated by the successful eradication of smallpox through vaccination [4]. Consequently, scientists worldwide are agreeing in development of effective COVID-19 vaccines, recognizing their potential to safe countless lives as a new tool in the battle against the virus [4].

In order to gain a deeper comprehension of how epidemic illnesses work and suggest more effective approaches to prevent their spread, mathematical models can be highly valuable. These models serve as helpful tools for predicting the patterns and progression of diseases, allowing us to implement strategies that can reduce the rate of infection and mortality. Recent advancements have introduced new mathematical models specifically designed to forecast disease dynamics and flatten the curves of infection and death [5,6]. Moreover, numerous compartmental mathematical models have been developed to explore the influence and significance of vaccination in combating various infectious diseases, as detailed in a range of studies [7–10].

Based on the existing literature, the focus of this study is to develop a new stochastic model that can analyzed the dynamics of COVID-19, taking into account the impact of vaccination. The proposed model incorporates a stochastic term to enhance its accuracy. The first objective of current research is to examine the transmission patterns of COVID-19, specifically in relation to Non-Pharmaceutical Interventions (NPIs) and the vaccination process. To establish the parameters of the model, actual pandemic cases in Pakistan are used for estimation. The study also presents the basic reproduction number and equilibrium points, along with conducting various fundamental analysis. The research findings from this study can be valuable for government authorities and public health agencies in formulating effective strategies to minimize the spread of future outbreaks.

This research paper is organized into different sections to provide a comprehensive analysis of the stochastic COVID-19 vaccination model. In Section 2, we present the mathematical modeling of this model, which involves describing the various factors and variables that influence the spread of the virus and the effectiveness of vaccinations. To further enhance our understanding, Section 3 reviews the application of Legendre polynomials and the spectral method in this context, as these mathematical tools have proven valuable in analyzing complex systems. In Section 4, we briefly discuss the basic reproduction number, an important metric in epidemiology, and conduct a stability analysis to assess the robustness of our model. In Section 5, we delve into the numerical results obtained from our simulations and discuss their implications for COVID-19 vaccination strategies. Finally, we conclude our research paper by summarizing our findings and highlighting the key takeaways in the last section.

## 2. Stochastic COVID-19 vaccine model

In this section, we focus on modeling a stochastic COVID-19 vaccination model to investigate the impact of certain non-pharmaceutical interventions (NPIs), specifically social distancing in combination with vaccination. Although the COVID-19 vaccine is currently in an experimental phase and only available to a limited extent, it plays a crucial role in controlling the pandemic alongside other pharmaceutical mediation. To construct mathematical model, we divide the total population into distinct classes: susceptible individuals (S(t)), vaccinated individuals (V(t)), exposed individuals (E(t)), asymptomatic infected individuals ($I_A(t)$), the symptomatic infected individuals (I(t)) and recovered from infection is denoted by (R(t)). Where, total population (N(t)) is the sum of all above classes.

The proposed model for the stochastic COVID-19 vaccine can be represented as a set of stochastic differential equations, which are nonlinear in nature. Mathematically, this model describes the relationship between various factors involved in the vaccine's effectiveness and its impact on the spread of the disease. By using these equations, we can better understand and predict how the vaccine will interact with the virus and the human immune system, providing valuable insights into its potential efficacy.

$$\begin{cases} \frac{dS}{dt} = \Lambda + \psi V - \frac{\beta(I+\beta_A I_A)S}{N} - (\mu+\omega_1)S, \\ \frac{dE}{dt} = \frac{\beta(I+\beta_A I_A)S}{N} - (\mu+\kappa)E, \\ \frac{dI}{dt} = \kappa(1-r)E - (\mu+\mu_1+\phi_1)I, \\ \frac{dI_A}{dt} = r\kappa E - (\mu+\phi_2)I_A, \\ \frac{dV}{dt} = \omega_1 S - (\psi+\mu)V, \\ \frac{dR}{dt} = \phi_1 I + \phi_2 I_A - \mu R. \end{cases} \tag{1}$$

with positive initial values $\lambda_i; i = 1, 2, ..., 6$, respectively for each class.

In the considered system described by Eqs. 1, the parameter $\Lambda$ represents the assumed birth rate, whereas $\mu$ denotes the natural death rate within each class of the model. The rate at which susceptible individuals receive vaccinations is represented by $\omega_1$, and those who have been vaccinated become susceptible again at a rate of $\psi$. Latent individuals become infected at a rate of $\kappa(1-r)$, where the remaining individuals (proportion $r$) join the group of asymptomatic infection. Where parameter $\mu_1$ shows the COVID-19 convinced mortality rate, while $\phi_1$ and $\phi_2$ indicate the rate at which both symptomatically and asymptomatically infected individuals recover. The transmission of the disease is characterized by $\beta$, and the transmissibility coefficient of asymptomatic individuals is denoted by $\beta_A$.

It is expected that all the parameters have positive values.

In present research work, we implement the spectral method for the numerical solution of COVID-19 system. This method were initially applied for differential and integral system [11–13]. Moreover, for numerical solutions of different diseases models the proposed method are applied by authors [14–17].

Since infectious diseases are subject to randomness in terms of the nature of transmission, the deterministic COVID-19 model given in Eqs. 1 is perturbed by white noise to obtain a stochastic model given in form:

$$\begin{cases} \frac{dS}{dt} = \Lambda + \psi V - \frac{\beta(I+\beta_A I_A)S}{N} - (\mu+\omega_1)S + \phi S dB(t), \\ \frac{dE}{dt} = \frac{\beta(I+\beta_A I_A)S}{N} - (\mu+\kappa)E + \phi E dB(t), \\ \frac{dI}{dt} = \kappa(1-r)E - (\mu+\mu_1+\phi_1)I + \phi I dB(t), \\ \frac{dI_A}{dt} = r\kappa E - (\mu+\phi_2)I_A + \phi I_A dB(t), \\ \frac{dV}{dt} = \omega_1 S - (\psi+\mu)V + \phi V dB(t), \\ \frac{dR}{dt} = \phi_1 I + \phi_2 I_A - \mu R + \phi R dB(t). \end{cases} \tag{2}$$

In this study, we are focusing on the spectral method for obtaining the solution to a stochastic COVID-19 model described by Eqs. 2. In this model, $B(t)$ represents Brownian motion, which is a random process that exhibits erratic behavior over time. The parameter $\phi$ is referred the intensity of Brownian motion, which determines the degree of randomness or volatility in the system. By developing an approximate solution to this stochastic model, we aim to better understand and predict the dynamics of COVID-19.

## 3. Spectral Method

Before apply spectral method, to provide an preview of Legendre polynomials given in [18]. The $n^{th}$ order Legendre polynomials denoted by $P_n(\tau_a)$. Where the function $u(\tau_a)$ is approximated by:

$$u(\tau_a) = \sum_{i=0}^{n} u_i P_i(\tau_a) \tag{3}$$

Preprints (www.preprints.org) | NOT PEER-REVIEWED | Posted: 21 July 2023 doi:10.20944/preprints202307.1476.v1



$u_i$ indicates Legendre coefficients, $\tau_{ai}, i = 0, ..., n$ are collocation nodes and $P_n(\tau_a)$ denotes $n^{th}$-order. Where the Legendre polynomials are:

$$P_i(\tau_a) = \frac{1}{2^i}\sum_{a=0}^{[\frac{i}{2}]}(-1)^a\binom{i}{a}\binom{2(i-a)}{i}\tau^{i-2a}, \quad (i = 0, 1, ..., n), \quad \tau_a \in [-1, 1]. \tag{4}$$

$$\frac{i}{2} = \begin{cases} \frac{i}{2}, & i \quad \text{Even}, \\ \frac{i-1}{2}, & i \quad \text{Odd}. \end{cases}$$

Spectral method procedure we considered the Legendre-Gauss-Lobatto points $\{t_j\}_{j=0}^{N}$.
For this, taking integral on Eq. 2 from $[0, t]$.

$$\begin{cases} S(t) &= S(0) + \int_0^t \left(\Lambda + \psi V(s) - \frac{\beta(I(s)+\beta_A E(s))S(s)}{N} - (\mu + \omega_1)S(s)\right)ds + \int_0^t \phi S(s)dB(s), \\ E(t) &= E(0) + \int_0^t \left(\frac{\beta(I(s)+\beta_A I_A(s))S(s)}{N} - (\kappa + \mu)E(s)\right)ds + \int_0^t \phi E(s)dB(s), \\ I(t) &= I(0) + \int_0^t \left((1-r)\kappa E(s) - (\mu + \mu_1 + \phi_1)I(s)\right)ds + \int_0^t \phi I(s)dB(s), \\ I_A(t) &= I_A(0) + \int_0^t \left(r\kappa E(s) - (\mu + \phi_2)I_A(s)\right)ds + \int_0^t \phi I_A(s)dB(s), \\ V(t) &= V(0) + \int_0^t \left(\omega_1 S(s) - (\psi + \mu)V(s)\right)ds + \int_0^t \phi V(s)dB(s), \\ R(t) &= R(0) + \int_0^t \left(\phi_1 I(s) + \phi_2 I_A(s) - \mu R(s)\right)ds + \int_0^t \phi R(s)dB(s). \end{cases} \tag{5}$$

where $S(0), E(0), I(0), I_A(0), V(0), R(0)$ are initial conditions on the functions of each class respectively. To convert the present interval to $[-1, 1]$ interval, we transform $s$ like: $s = \frac{t}{2}(1 + \varpi)$, then Eqs. 5 becomes:

$$\begin{aligned} S(t) &= S(0) + \frac{1}{2}t\int_{-1}^{1}\Bigg(\Lambda + \psi V(\frac{t(1+\varpi)}{2}) - \frac{\beta\big(I(\frac{t(1+\varpi)}{2}) + \beta_A E(\frac{t(1+\varpi)}{2})\big)S(\frac{t(1+\varpi)}{2})}{N} \\ &\quad - (\mu + \omega_1)S(\frac{t(1+\varpi)}{2})\Bigg)d\varpi + \frac{1}{2}t\int_{-1}^{1}\phi S\left(\frac{t(1+\varpi)}{2}\right)dB(\varpi), \\ E(t) &= E(0) + \frac{1}{2}t\int_{-1}^{1}\left(\frac{\beta\big(I(\frac{t(1+\varpi)}{2}) + \beta_A I_A(\frac{t(1+\varpi)}{2})\big)S(\frac{t(1+\varpi)}{2})}{N} - (\kappa + \mu)E(\frac{t(1+\varpi)}{2})\right)d\varpi \\ &\quad + \frac{1}{2}t\int_{-1}^{1}\phi E\left(\frac{t(1+\varpi)}{2}\right)dB(\varpi), \\ I(t) &= I(0) + \frac{1}{2}t\int_{-1}^{1}\left((1-r)\kappa E(\frac{t(1+\varpi)}{2}) - (\mu + \mu_1 + \phi_1)I(\frac{t(1+\varpi)}{2})\right)d\varpi \\ &\quad + \frac{1}{2}t\int_{-1}^{1}\phi I\left(\frac{t(1+\varpi)}{2}\right)dB(\varpi), \\ I_A(t) &= I_A(0) + \frac{1}{2}t\int_{-1}^{1}\left(r\kappa E(\frac{t(1+\varpi)}{2}) - (\mu + \phi_2)I_A(\frac{t(1+\varpi)}{2})\right)d\varpi \\ &\quad + \frac{1}{2}t\int_{-1}^{1}\phi I_A\left(\frac{t(1+\varpi)}{2}\right)dB(\varpi), \\ V(t) &= V(0) + \frac{1}{2}t\int_{-1}^{1}\left(\omega_1 S(\frac{t(1+\varpi)}{2}) - (\psi + \mu)V(\frac{t(1+\varpi)}{2})\right)d\varpi \\ &\quad + \frac{1}{2}t\int_{-1}^{1}\phi V\left(\frac{t(1+\varpi)}{2}\right)dB(\varpi), \\ R(t) &= R(0) + \frac{1}{2}t\int_{-1}^{1}\left(\phi_1 I(\frac{t(1+\varpi)}{2}) + \phi_2 I_A(\frac{t(1+\varpi)}{2}) - \mu R(\frac{t(1+\varpi)}{2})\right)d\varpi \\ &\quad + \frac{1}{2}t\int_{-1}^{1}\phi R\left(\frac{t(1+\varpi)}{2}\right)dB(\varpi). \end{aligned} \tag{6}$$

Preprints (www.preprints.org) | NOT PEER-REVIEWED | Posted: 21 July 2023 doi:10.20944/preprints202307.1476.v1



where the semi discretized spectral system Eqs. 6 are:

$$
\begin{aligned}
S(t) &= S(0) + \frac{1}{2}t\sum_{k=0}^{N}\Bigg(\Lambda + \psi V(\frac{t(1+\varpi)}{2}) - \frac{\beta(I(\frac{t(1+\varpi)}{2}) + \beta_A E(\frac{t(1+\varpi)}{2}))S(\frac{t(1+\varpi)}{2})}{N} \\
&\quad - (\mu+\omega_1)S(\frac{t(1+\varpi)}{2})\Bigg)\omega_k + \frac{1}{2}t\sum_{k=0}^{N}\phi S\Bigg(\frac{t(1+\varpi)}{2}\Bigg)\omega_k^*, \\
E(t) &= E(0) + \frac{1}{2}t\sum_{k=0}^{N}\Bigg(\frac{\beta(I(\frac{t(1+\varpi)}{2}) + \beta_A I_A(\frac{t(1+\varpi)}{2}))S(\frac{t(1+\varpi)}{2})}{N} - (\kappa+\mu)E(\frac{t(1+\varpi)}{2})\Bigg)\omega_k \\
&\quad + \frac{1}{2}t\sum_{k=0}^{N}\phi E\Bigg(\frac{t(1+\varpi)}{2}\Bigg)\omega_k^*, \\
I(t) &= I(0) + \frac{1}{2}t\sum_{k=0}^{N}\Bigg((1-r)\kappa E(\frac{t(1+\varpi)}{2}) - (\mu+\mu_1+\phi_1)I(\frac{t(1+\varpi)}{2})\Bigg)\omega_k \\
&\quad + \frac{1}{2}t\sum_{k=0}^{N}\phi I\Bigg(\frac{t(1+\varpi)}{2}\Bigg)\omega_k^*, \\
I_A(t) &= I_A(0) + \frac{1}{2}t\sum_{k=0}^{N}\Bigg(r\kappa E(\frac{t(1+\varpi)}{2}) - (\mu+\phi_2)I_A(\frac{t(1+\varpi)}{2})\Bigg)\omega_k \\
&\quad + \frac{1}{2}t\sum_{k=0}^{N}\phi I_A\Bigg(\frac{t(1+\varpi)}{2}\Bigg)\omega_k^*, \\
V(t) &= V(0) + \frac{1}{2}t\sum_{k=0}^{N}\Bigg(\omega_1 S(\frac{t(1+\varpi)}{2}) - (\psi+\mu)V(\frac{t(1+\varpi)}{2})\Bigg)\omega_k \\
&\quad + \frac{1}{2}t\sum_{k=0}^{N}\phi V\Bigg(\frac{t(1+\varpi)}{2}\Bigg)\omega_k^*, \\
R(t) &= R(0) + \frac{1}{2}t\sum_{k=0}^{N}\Bigg(\phi_1 I(\frac{t(1+\varpi)}{2}) + \phi_2 I_A(\frac{t(1+\varpi)}{2}) - \mu R(\frac{t(1+\varpi)}{2})\Bigg)\omega_k \\
&\quad + \frac{1}{2}t\sum_{k=0}^{N}\phi R\Bigg(\frac{t(1+\varpi)}{2}\Bigg)\omega_k^*. \qquad (7)
\end{aligned}
$$

where the weight function refer [12,13], for Eq. 1 is given by

$$\omega_k = \frac{2}{[L'_{1+N}(s_k)]^2(1-s_k^2)}, \quad where \quad 0 \le k \le N.$$

$L$ is the Lagrange polynomials.

Also the weight function for Eq. 2 is given by

$$\omega_k^* = \sqrt{\omega_k} \times randn(1, N), \quad 0 \le k \le N.$$

Now the spectral solution of each $S, E, I, I_A, V$ and $R$ by using the above Eq. 5

$$
\begin{aligned}
&S = \sum_{n=0}^{N} S_n P_n(t), \quad E = \sum_{n=0}^{N} E_n P_n(t), \quad I = \sum_{n=0}^{N} I_n P_n(t), \quad I_A = \sum_{n=0}^{N} (I_A)_n P_n(t), \\
&V = \sum_{n=0}^{N} V_n P_n(t), \quad R = \sum_{n=0}^{N} R_n P_n(t). \qquad (8)
\end{aligned}
$$

Legendre coefficients of each of functions $S(t)$, $E(t)$, $I(t)$, $I_A(t)$, $V(t)$ and $R(t)$ are in the form: $S_n, E_n, I_n, (I_A)_n, V_n, R_n$, respectively. Now using the solution Eqs. 9 becomes:

$$
\begin{aligned}
\sum_{n=0}^{N} S_n P_n(t) &= \sum_{n=0}^{N} S_n P_n(0) + \frac{1}{2} t \sum_{k=0}^{N} \Bigg( \Lambda + \psi \sum_{n=0}^{N} V_n P_n(\zeta_k) \\
&- \frac{\beta\big( \sum_{n=0}^{N} I_n P_n(\zeta_k) + \beta_A \sum_{n=0}^{N} (I_A)_n P_n(\zeta_k) \big) \sum_{n=0}^{N} S_n P_n(\zeta_k)}{N} \\
&- (\mu + \omega_1) \sum_{n=0}^{N} S_n P_n(\zeta_k) \Bigg) \omega_k + \frac{1}{2} t \sum_{k=0}^{N} \phi \sum_{n=0}^{N} S_n P_n(\zeta_k) \omega_k^*, \\
\sum_{n=0}^{N} E_n P_n(t) &= \frac{1}{2} t \sum_{k=0}^{N} \Bigg( \frac{\beta\big( \sum_{n=0}^{N} I_n P_n(\zeta_k) + \beta_A \sum_{n=0}^{N} (I_A)_n P_n(\zeta_k) \big) \sum_{n=0}^{N} S_n P_n(\zeta_k)}{N} \\
&- (\kappa + \mu) \sum_{n=0}^{N} E_n P_n(\zeta_k) \Bigg) \omega_k + \frac{1}{2} t \sum_{k=0}^{N} \phi \sum_{n=0}^{N} E_n P_n(\zeta_k) \omega_k^* + \sum_{n=0}^{N} E_n P_n(0), \\
\sum_{n=0}^{N} I_n P_n(t) &= \sum_{n=0}^{N} I_n P_n(0) + \frac{1}{2} t \sum_{k=0}^{N} \Bigg( (1 - r)\kappa \sum_{n=0}^{N} E_n P_n(\zeta_k) \\
&- (\mu + \mu_1 + \phi_1) \sum_{n=0}^{N} I_n P_n(\zeta_k) \Bigg) \omega_k + \frac{1}{2} t \sum_{k=0}^{N} \phi \sum_{n=0}^{N} I_n P_n(\zeta_k) \omega_k^*, \\
\sum_{n=0}^{N} (I_A)_n P_n(t) &= \sum_{n=0}^{N} (I_A)_n P_n(0) + \frac{1}{2} t \sum_{k=0}^{N} \Bigg( r\kappa \sum_{n=0}^{N} E_n P_n(\zeta_k) - (\mu + \phi_2) \sum_{n=0}^{N} (I_A)_n P_n(\zeta_k) \Bigg) \omega_k \\
&+ \frac{1}{2} t \sum_{k=0}^{N} \phi \sum_{n=0}^{N} (I_A)_n P_n(\zeta_k) \omega_k^*, \\
\sum_{n=0}^{N} V_n P_n(t) &= \sum_{n=0}^{N} V_n P_n(0) + \frac{1}{2} t \sum_{k=0}^{N} \Bigg( \omega_1 \sum_{n=0}^{N} S_n P_n(\zeta_k) - (\psi + \mu) \sum_{n=0}^{N} V_n P_n(\zeta_k) \Bigg) \omega_k \\
&+ \frac{1}{2} t \sum_{k=0}^{N} \phi \sum_{n=0}^{N} V_n P_n(\zeta_k) \omega_k^*, \\
\sum_{n=0}^{N} R_n P_n(t) &= \sum_{n=0}^{N} R_n P_n(0) + \frac{1}{2} t \sum_{k=0}^{N} \Bigg( \phi_1 \sum_{n=0}^{N} I_n P_n(\zeta_k) + \phi_2 \sum_{n=0}^{N} (I_A)_n P_n(\zeta_k) \\
&- \mu \sum_{n=0}^{N} R_n P_n(\zeta_k) \Bigg) \omega_k + \frac{1}{2} t \sum_{k=0}^{N} \phi \sum_{n=0}^{N} R_n P_n(\zeta_k) \omega_k^*. \qquad (9)
\end{aligned}
$$

We take $\zeta_k = (\frac{t(1+\varpi)}{2})$. The proposed system Eqs. 9 gives of $6N + 6$ of unknowns in which $6N$ nonlinear equations. Using initial conditions say:

$$
\begin{aligned}
&\textstyle\sum_{n=0}^{N} S_n P_n(0) = \lambda_1, \quad \sum_{n=0}^{N} E_n P_n(0) = \lambda_2, \quad \sum_{n=0}^{N} I_n P_n(0) = \lambda_3. \\
&\textstyle\sum_{n=0}^{N} (I_A)_n P_n(0) = \lambda_4, \quad \sum_{n=0}^{N} V_n P_n(0) = \lambda_5, \quad \sum_{n=0}^{N} R_n P_n(0) = \lambda_6. \qquad (10)
\end{aligned}
$$

Eqs. 10 and Eqs. 9 of a system of $(6N + 6)$ equations. Therefore, the solving the above two systems gives the solution of corresponding all unknowns. In last using the unknown values in Eqs. 8, and get a solution to the model given in Eqs. 2.

## 4. Stability Analysis

Stability analysis is a crucial tool for investigating the behavior of a dynamical system. In this particular section, we delve into the examination of the stability of equilibrium solution. These equilibrium solutions are associated with both deterministic and stochastic systems, which are represented by equations labeled as Eqs. 1 and Eqs. 2 respectively. By studying the stability of

Preprints (www.preprints.org) | NOT PEER-REVIEWED | Posted: 21 July 2023 doi:10.20944/preprints202307.1476.v1



these solutions, we gain insights into how the system's dynamics unfold over time, accounting for both deterministic and random influences.

The COVID-19 model described by Eqs. 1 can have up to two equilibrium solutions. The first one, called the infection-free equilibrium $E_0$, represents a steady state solution where there is no disease in the population. The second equilibrium solution is known as the endemic equilibrium, which occurs when the disease persists within the population.

### 4.1. Basic reproductive number ($\mathscr{R}_0$) by Next-generation matrices method

The system of Eqs. 2 provide the simple vaccination model that describes the coronavirus disease. Now the infectious subsystem of Eqs. 2 gives that,

$$\begin{cases} \frac{dE}{dt} = \frac{\beta S(I+\beta_A I_A)}{N} - (\mu+\kappa)E, \\ \frac{dI}{dt} = (1-r)\kappa E - (\mu+\mu_1+\phi_1)I, \\ \frac{dI_A}{dt} = r\kappa E - (\mu+\phi_2)I_A, \\ \frac{dV}{dt} = \omega_1 S - (\psi+\mu)V, \end{cases} \tag{11}$$

So the jacobian matrix of the Eqs. 11 is computed as

$$J(E,I,I_A,V) = \begin{bmatrix} -\kappa-\mu & \beta S & \beta\beta_A S & 0 \\ (1-r)\kappa & -(\mu-\mu_1-\phi_1 & 0 & 0 \\ r\kappa & 0 & -\mu-\phi_2 & 0 \\ 0 & 0 & 0 & -\psi-\mu \end{bmatrix} \tag{12}$$

As seen below, the Jacobi matrix is split into two matrices

$$\Gamma = \begin{bmatrix} 0 & \beta S & \beta\beta_A S & 0 \\ 0 & 0 & 0 & 0 \\ 0 & 0 & 0 & 0 \\ 0 & 0 & 0 & 0 \end{bmatrix}$$

$$\Delta = \begin{bmatrix} -\kappa-\mu & 0 & 0 & 0 \\ (1-r)\kappa & -(\mu-\mu_1-\phi_1 & 0 & 0 \\ r\kappa & 0 & -(\mu+\phi_2) & 0 \\ 0 & 0 & 0 & -\psi-\mu \end{bmatrix}$$

And the transition matrix inversion is

$$\Delta^{-1} = \begin{bmatrix} \frac{-1}{(\kappa+\mu)} & 0 & 0 & 0 \\ \frac{(-1+r)\kappa}{\left((\kappa+\mu)(\mu+\mu_1+\phi_1)\right)} & \frac{-1}{(\mu+\mu_1+\phi_1)} & 0 & 0 \\ \frac{-r\kappa}{\left((\kappa+\mu)(\mu+\phi_2)\right)} & 0 & \frac{-1}{(\mu+\phi_2)} & 0 \\ 0 & 0 & 0 & \frac{-1}{(\psi+\mu)} \end{bmatrix}$$

By analyzing the following classes instances, the basic reproductive equation ($\mathscr{R}_0$) may be constructed. Now the NGM with large domain is denoted by $D_L$ is given by:

$$D_L = -\Gamma\Delta^{-1} = \begin{bmatrix} \frac{-\beta S(-1+r)\kappa}{(\kappa+\mu)(\mu+\mu_1+\phi_1)} + \frac{\beta\beta_A S r\kappa}{(\kappa+\mu)(\mu+\phi_2)} & \frac{\beta S}{(\mu+\mu_1+\phi_1)} & \frac{\beta\beta_A S}{\mu+\phi_2} & 0 \\ 0 & 0 & 0 & 0 \\ 0 & 0 & 0 & 0 \\ 0 & 0 & 0 & 0 \end{bmatrix}$$

 doi:10.20944/preprints202307.1476.v1



In light of this, the basic reproduction formula for a matrix with a large domain is

$$\mathscr{R}_0 = trace(D_L) = \frac{-\beta S(-1+r)\kappa}{(\kappa+\mu)(\mu+\mu_1+\phi_1)} + \frac{\beta\beta_A S r\kappa}{(\kappa+\mu)(\mu+\phi_2)} \tag{13}$$

Following equation gives the reproduction number for the system given by Eqs. 1

$$\mathscr{R}_0 = \frac{\Lambda\beta(1-r)\kappa}{(\mu+\omega_1)(\kappa+\mu)(\mu+\mu_1+\phi_1)} + \frac{\Lambda\beta\beta_A r\kappa}{(\mu+\omega_1)(\kappa+\mu)(\mu+\phi_2)}. \tag{14}$$

**Theorem 4.1.** *If $\mathscr{R}_0 \leq 1$, then disease-free equilibrium $E_0$ is a stable solution for a system described by equations Eqs. 1 on the entire region $\mathbb{D}$, which means that disease will not be spread and the population will remain healthy. On the other hand, if $\mathscr{R}_0 > 1$, then the endemic equilibrium solution $E_1^*$ (with values $S^*$, $E^*$, $I^*$, $I_A^*$, $V^*$, and $R^*$) of the system described by equations Eqs. 1 is asymptotically stable on the region $\mathbb{D}$. This implies that the disease will persist in the population.*

$$\begin{aligned}
S^* &= \frac{(\kappa+\mu)(\mu+\mu_1+\phi_1)(\mu+\phi_2)N}{\beta((1-r)\kappa(\mu+\phi_2)-\beta_A r\kappa(\mu+\mu_1+\phi_1))},\\
E^* &= \frac{(\mu+\mu_1+\phi_1)^2}{(\kappa(1-r)(\mu+\mu_1+\phi_1-1))},\\
I^* &= \frac{(\mu+\mu_1+\phi_1)}{(\mu+\mu_1+\phi_1-1)},\\
I_A^* &= \frac{r\kappa(\mu+\mu_1+\phi_1)^2}{(\kappa(1-r)(\mu+\phi_2)(\mu+\mu_1+\phi_1-1))},\\
V^* &= \frac{\omega_1(\mu+\mu_1+\phi_1)N(\kappa+\mu)(\mu+\phi_2)}{\beta((1-r)\kappa(\mu+\phi_2)-\beta_A r\kappa(\mu+\mu_1+\phi_1))(\mu+\psi)},\\
R^* &= \frac{(\mu+\mu_1+\phi_1)\Big(((-1+r)\kappa\mu+\phi_2((-1+r)\kappa-r\kappa))\phi_1-\phi_2 r\kappa(\mu+\mu_1)\Big)}{((-1+r)\kappa(\mu+\mu_1+\phi_1-1)(\mu+\phi_2)\mu)}
\end{aligned} \tag{15}$$

**Proof.** The endemic equilibrium $E_1^*$ of system given by Eq. 1, has stationary system is given by:

$$\begin{aligned}
&\Lambda+\psi V^* - \frac{\beta(I^*+\beta_A I_A^*)S^*}{N} - (\mu+\omega_1)S^* = 0,\\
&\frac{\beta(I^*+\beta_A I_A^*)S^*}{N} - (\mu+\kappa)E^* = 0,\\
&\kappa(1-r)E^* - (\mu+\mu_1+\phi_1)I^* = 0,\\
&r\kappa E^* - (\mu+\phi_2)I_A^* = 0,\\
&\omega_1 S^* - (\psi+\mu)V^* = 0,\\
&\phi_1 I^* + \phi_2 I_A^* - \mu R^* = 0.
\end{aligned} \tag{16}$$

To solve system in Eq. 16. We will discuss two major cases:

a. infected classes $I$ and $I_A$ equal to zero
b. $I$ and $I_A$ greater than zero.

(a): If $I = 0 = I_A$: then from the last equation of Eqs. 16, we get $R^* = 0$, where from equation number four of Eqs. 16, we get $E^* = 0$, and using equation first, we get $S^* = \Lambda/(\mu+\omega_1)$. Similarly from the fifth equation we get $V = 0$. Therefore, we get the disease free equilibrium $E_1^* = (\Lambda/(\mu+\omega_1), 0, 0, 0, 0, 0, )$, having a case $\mathscr{R}_0 < 1$.

(b): If $I^* > 0$ and $I_A^* > 0$, for the lake of calculation using Maple-13 software to found the proposed endemic equilibrium $E_1^*$. In this case should be $\mathscr{R}_0 > 1$.

□

*Preprints* (www.preprints.org) | NOT PEER-REVIEWED | Posted: 21 July 2023 doi:10.20944/preprints202307.1476.v1



**Lemma 4.2.** *Total region say $\mathbb{D}$ is positive invariance set for the proposed model given in Eqs. 1.*

**Proof.** For $N(t) = S + E + I + I_A + V + R$, then using model Eqs. 1, we get:

$$\frac{d}{dt}N(t) = \Lambda - (\mu + \omega_1)N(t) - \mu_1 I - \psi V. \tag{17}$$

$$\frac{d}{dt}N(t) \leq \Lambda - (\mu + \omega_1)N(t). \tag{18}$$

Therefore, Eq. 18 takes the form:

$$N(t) \leq \frac{\Lambda}{(\mu + \omega_1)} + N(0)e^{-(\mu+\omega_1)t} \leq \frac{\Lambda}{(\mu + \omega_1)}.$$

Hence in the total region $\mathbb{D}$ the system Eq. 1 is positively invariant. □

The following lemma are proved by using method refer [19],.

**Lemma 4.3.** *The solution of system Eqs. 1 $(S(t), E(t), I(t), I_A(t), V(t), R(t))$ has above properties for each initial condition $\big(S(0), E(0), I(0), I_A(0), V(0), R(0)\big) \in \mathbb{R}^6$:*

$$\lim_{t\to\infty} \frac{1}{t}\int_0^t \phi S(u)dW(u) = 0,$$

*and similarly for each class.*

**Definition 4.4.** *Individuals that are infected in population $I$ and $I_A$ are termed extinctive for model Eqs. 2 if and only if $\lim_{t\to\infty} I(t) = 0 = \lim_{t\to\infty} I_A(t) = 0$.*

**Theorem 4.5.** *Since,* $\max\left\{\left(\frac{\beta(\mu+\omega_1)}{\Lambda} + \frac{\beta\beta_A(\mu+\omega_1)}{\Lambda}\right), \left(\frac{\beta^2}{2(\kappa+\mu)(\mu+\mu_1+\phi_1)} + \frac{\beta^2\beta_A^2}{2(\kappa+\mu)(\mu+\phi_2)}\right)\right\} < \phi^2$ *or* $\left(\frac{\beta(\mu+\omega_1)}{\Lambda} + \frac{\beta\beta_A(\mu+\omega_1)}{\Lambda}\right) > \phi^2$ *with $\bar{\mathscr{R}}_0 < 1$, then both the infected classes $I$ and $I_A$ of Eq. 2 are exponentially tends to zero. Conversely, if $\bar{\mathscr{R}}_0 > 1$, the each class of the model Eqs. 2 are present, where*

$$\bar{\mathscr{R}}_0 = \mathscr{R}_0 - \left(\frac{\big(\phi\Lambda(1-r)\kappa\big)^2}{(\mu+\omega_1)^2} + \frac{\big(\phi\Lambda r\kappa\big)^2}{(\mu+\omega_1)^2}\right)$$

**Proof.** Suppose the solution of the proposed vaccination model Eq. (2) in the form of $\{S, E, I, I_A, V, R\}$ along with initial conditions $\{S(0), E(0), I(0), I_A(0), V(0), R(0)\}$. Also assume that $I_N = I + I_A$, then by using Itô formula we get:

$$\begin{aligned} d\ln I_N(t) = &\left(\frac{\beta S(1-r)\kappa}{N} - (\kappa+\mu)(\mu+\mu_1+\phi_1) - \frac{\phi^2 S^2}{2}\right)dt + \phi S dW(t) \\ &+ \left(\frac{\beta\beta_A S r\kappa}{N} - (\kappa+\mu)(\mu+\phi_2) - \frac{\phi^2 S^2}{2}\right)dt + \phi S dW(t). \end{aligned} \tag{19}$$

Apply integral from 0 to $t$, we have

$$\begin{aligned} \ln I_N(t) = \ln I_N(0) &+ \int_0^t \left(\frac{\beta S(1-r)\kappa}{N} - (\kappa+\mu)(\mu+\mu_1+\phi_1) - \frac{\phi^2 S^2}{2}\right)dt + \int_0^t \phi S dW(t) \\ &+ \int_0^t \left(\frac{\beta\beta_A S r\kappa}{N} - (\kappa+\mu)(\mu+\phi_2) - \frac{\phi^2 S^2}{2}\right)dt + \int_0^t \phi S dW(t). \end{aligned} \tag{20}$$

here we discuss the two cases, if $\phi^2 > \left(\frac{\beta(\mu+\omega_1)}{\Lambda} + \frac{\beta\beta_A(\mu+\omega_1)}{\Lambda}\right)$, then

$$\begin{aligned}\ln I_N(t) \leq \ln I_N(0) + \left(\frac{\beta^2(1-r)\kappa}{\phi^2} - (\kappa+\mu)(\mu+\mu_1+\phi_1)\right)t + \int_0^t \phi S dW(t)\\ + \left(\frac{\beta^2\beta_A^2 r\kappa}{\phi^2} - (\kappa+\mu)(\mu+\phi_2)\right)t + \int_0^t \phi S dW(t)\end{aligned} \tag{21}$$

Divide Eq. (21) by $t > 0$, then

$$\begin{aligned}\frac{\ln I_N(t)}{t} \leq \frac{\ln I_N(0)}{t} + \left(\frac{\beta^2(1-r)\kappa}{\phi^2} - (\kappa+\mu)(\mu+\mu_1+\phi_1)\right) + \frac{1}{t}\int_0^t \phi S dW(t)\\ + \left(\frac{\beta^2\beta_A^2 r\kappa}{\phi^2} - (\kappa+\mu)(\mu+\phi_2)\right) + \frac{1}{t}\int_0^t \phi S dW(t)\end{aligned} \tag{22}$$

By taking $\lim_{t\to\infty}$ and using Lemma 4.3, then Eq. (22) converted to

$$\lim_{t\to\infty}\frac{\ln I_N(t)}{t} \leq -\left((\kappa+\mu)(\mu+\mu_1+\phi_1) - \frac{\beta^2(1-r)\kappa}{\phi^2}\right) - \left((\kappa+\mu)(\mu+\phi_2) - \frac{\beta^2\beta_A^2 r\kappa}{\phi^2}\right) < 0.$$

Which shows, $\lim_{t\to\infty} I_N(t) = 0$.

The second case, when $\phi^2 < \left(\frac{\beta(\mu+\omega_1)}{\Lambda} + \frac{\beta\beta_A(\mu+\omega_1)}{\Lambda}\right)$, and using Eq. (20) we get

$$\begin{aligned}\ln I_N(t) \leq \ln I_N(0) + \left(\frac{\beta\Lambda(1-r)\kappa}{\mu+\omega_1} - \frac{(\phi\Lambda(1-r)\kappa)^2}{(\mu+\omega_1)^2} - (\kappa+\mu)(\mu+\mu_1+\phi_1)\right)t\\ + \left(\frac{\beta\beta_A\Lambda r\kappa}{\mu+\omega_1} - \frac{(\phi\Lambda r\kappa)^2}{(\mu+\omega_1)^2} - (\kappa+\mu)(\mu+\phi_2)\right)t + 2\int_0^t \phi S dW(t)\end{aligned} \tag{23}$$

Dividing Eqs. (23) by $t$ where $t > 0$ we obtain

$$\begin{aligned}\frac{1}{t}\ln I_N(t) \leq \frac{1}{t}\ln I_N(0) + (\kappa+\mu)(\mu+\mu_1+\phi_1)\Bigg(\frac{\beta\Lambda(1-r)\kappa}{(\mu+\omega_1)(\mu+\mu_1+\phi_1)(\kappa+\mu)}\\ - \frac{(\phi\Lambda(1-r)\kappa)^2}{(\kappa+\mu)(\mu+\omega_1)^2(\mu+\mu_1+\phi_1)} - 1\Bigg)\\ + (\kappa+\mu)(\mu+\phi_2)\left(\frac{\beta\beta_A\Lambda r\kappa}{(\mu+\omega_1)(\kappa+\mu)(\mu+\phi_2)} - \frac{(\phi\Lambda r\kappa)^2}{(\mu+\omega_1)^2(\kappa+\mu)(\mu+\phi_2)} - 1\right)\\ + \frac{2}{t}\int_0^t \phi S dW(t)\end{aligned} \tag{24}$$

Again by taking $\lim_{t\to\infty}$ and use Lemma 4.3, Eq. (24) becomes

$$\lim_{t\to\infty}\frac{\ln I_N(t)}{t} \leq (\kappa+\mu)(\mu+\mu_1+\phi_1)(\mu+\phi_2)(\bar{\mathscr{R}}_0 - 1).$$

When $\bar{\mathscr{R}}_0 < 1$, then

$$\lim_{t\to\infty}\frac{1}{t}\ln I_N(t) < 0.$$

Which shows that $\lim_{t\to\infty} I_N(t) = 0$.

□

 doi:10.20944/preprints202307.1476.v1



## 5. Numerical Results

Current section focuses on presenting some numerical problems and their corresponding graphical results. The numerical results are captured and explained for both deterministic system Eqs. 1 and the stochastic system Eqs. 2. To find these numerical results, the spectral collocation method is employed. The obtained results are then visualized in Figures 1–8. The computations for this study are performed on a personal computer using Maple and Matlab software. To simplify the calculations, each initial value is assumed to be equal to 1.

**Figure 1** Following parameter values are assumed for deterministic system Eqs. 1 as $\Lambda = 6, \beta = 1, \beta_A = 1, \mu = 1, \mu_1 = 0.9, \phi_1 = 0.4958, \phi_2 = 0.6110, \kappa = 3.871, r = 0.8, \omega_1 = 0.001, \psi = 0.0233$. The computations gives reproduction number becomes $\mathscr{R}_0 < 1$, by using given parameter values. By using theorem 4.1, we see the model Eqs. 1 has stable infectious free equilibrium $E_0(6,0,0,0,0,0)$ where $S(t)$ is in the form $\Lambda/\mu = 6$.

**Figure 2** If we change $\beta = 2, \beta_A = 0.7$ and $\omega_1 = 0.1$ and remaining the same as in Figure 1. Then we got $\mathscr{R}_0 > 1$ and using theorem 4.1 the model Eqs. 1 has stable endemic equilibrium and all the compartments are then zero as given in Figure 2.

**Figure 3** When we chosen parameter values $\Lambda = 6, \beta = 1, \beta_A = 1, \mu = 1, \mu_1 = 0.9, \phi_1 = 0.4958, \phi_2 = 0.6110, \kappa = 3.871, r = 0.8, \omega_1 = 0.001, \psi = 0.0233, \phi = 0.7$ for stochastic system Eqs. 2. The above simulation shows that $\phi^2 > \max\left\{\left(\frac{\beta(\mu+\omega_1)}{\Lambda} + \frac{\beta\beta_A(\mu+\omega_1)}{\Lambda}\right), \left(\frac{\beta^2}{2(\kappa+\mu)(\mu+\mu_1+\phi_1)} + \frac{\beta^2\beta_A^2}{2(\kappa+\mu)(\mu+\phi_2)}\right)\right\}$ and $\bar{\mathscr{R}}_0 < 1$ along with theorem 4.5 the infected classes of model Eqs. 2 becomes zero.

**Figure 4** Choose $\beta = 2, \beta_A = 0.7$ and $\omega_1 = 0.1$ and remaining the same parameter values of Figure 3, then the stochastic model Eqs. 2, satisfy $\phi^2 < \max\left\{\left(\frac{\beta(\mu+\omega_1)}{\Lambda} + \frac{\beta\beta_A(\mu+\omega_1)}{\Lambda}\right), \left(\frac{\beta^2}{2(\kappa+\mu)(\mu+\mu_1+\phi_1)} + \frac{\beta^2\beta_A^2}{2(\kappa+\mu)(\mu+\phi_2)}\right)\right\}$, with $\bar{\mathscr{R}}_0 > 1$, using theorem 4.5, shows that each class are presents of Eqs. 2, this can be performed in Figure 4.

**Figure 5** Present figure show the comparison of the solutions Eqs. 1 and Eqs. 2 for each classes, where using parameter values $\Lambda = 6, \beta = 1, \beta_A = 1, \mu = 1, \mu_1 = 0.9, \phi_1 = 0.4958, \phi_2 = 0.6110, \kappa = 3.871, r = 0.8, \omega_1 = 0.001, \psi = 0.0233, \phi = 0.7$. The simple computation shows that for model Eqs. 1 $\mathscr{R}_0 < 1$, where for stochastic model Eqs. 2 $\max\left\{\left(\frac{\beta(\mu+\omega_1)}{\Lambda} + \frac{\beta\beta_A(\mu+\omega_1)}{\Lambda}\right), \left(\frac{\beta^2}{2(\kappa+\mu)(\mu+\mu_1+\phi_1)} + \frac{\beta^2\beta_A^2}{2(\kappa+\mu)(\mu+\phi_2)}\right)\right\} < \phi^2$ with $\bar{\mathscr{R}}_0 < 1$. Using the theorems 4.1 and 4.5, we see both the systems satisfy the disease free equilibriums.

**Figure 6** Comparison of both models given in Eqs. 1 and Eqs. 2 for each classes, using following values of parameter $\beta = 2, \beta_A = 0.7$ and $\omega_1 = 0.1$ and remaining the same parameter values as in Figure 5. Using such parameter values the Eqs. 1 $\mathscr{R}_0 > 1$, also for stochastic model Eqs. 2 $\max\left\{\left(\frac{\beta(\mu+\omega_1)}{\Lambda} + \frac{\beta\beta_A(\mu+\omega_1)}{\Lambda}\right), \left(\frac{\beta^2}{2(\kappa+\mu)(\mu+\mu_1+\phi_1)} + \frac{\beta^2\beta_A^2}{2(\kappa+\mu)(\mu+\phi_2)}\right)\right\} > \phi^2$ with $\bar{\mathscr{R}}_0 > 1$. Using the theorems 4.1 and 4.5, we see both the systems satisfy endemic equilibriums.

**Figure 7** Above same parameter values as given in Figure 5 to compare both the deterministic and stochastic solutions.

**Figure 8** The same parameter values as given in Figure 6 to compare both the deterministic and stochastic solutions.

 doi:10.20944/preprints202307.1476.v1



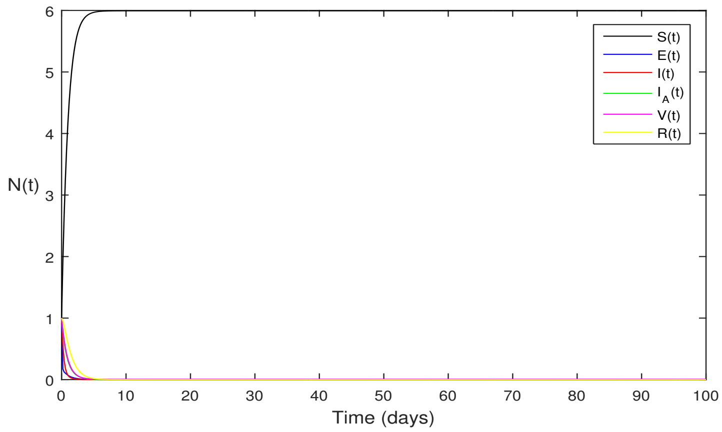


**Figure 1.** Deterministic COVID-19 system (1) using $\Lambda = 6, \beta = 1, \beta_A = 1, \mu = 1, \mu_1 = 0.9, \phi_1 = 0.4958, \phi_2 = 0.6110, \kappa = 3.871, r = 0.8, \omega_1 = 0.001, \psi = 0.0233$ that is $\mathscr{R}_0 < 1$.

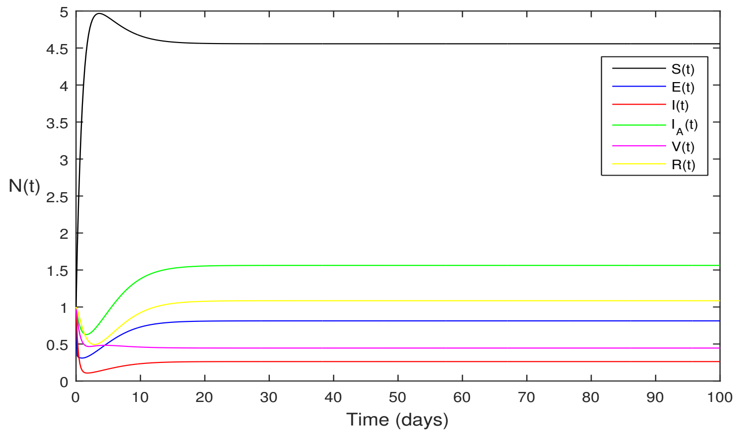


**Figure 2.** Deterministic system (1), with $\Lambda = 6, \beta = 2, \beta_A = 1.5, \mu = 1, \mu_1 = 0.9, \phi_1 = 0.4958, \phi_2 = 0.6110, \kappa = 3.871, r = 0.8, \omega_1 = 0.1, \psi = 0.0233$ that is $\mathscr{R}_0 > 1$.

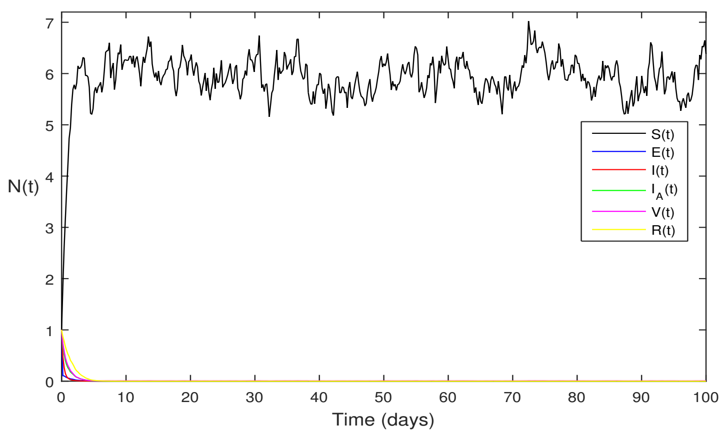


**Figure 3.** Stochastic system Eqs. 2, with $\Lambda = 6, \beta = 1, \beta_A = 1, \mu = 1, \mu_1 = 0.9, \phi_1 = 0.4958, \phi_2 = 0.6110, \kappa = 3.871, r = 0.8, \omega_1 = 0.001, \psi = 0.0233, \phi = 0.7$ where $\bar{\mathscr{R}}_0 < 1$.

 doi:10.20944/preprints202307.1476.v1



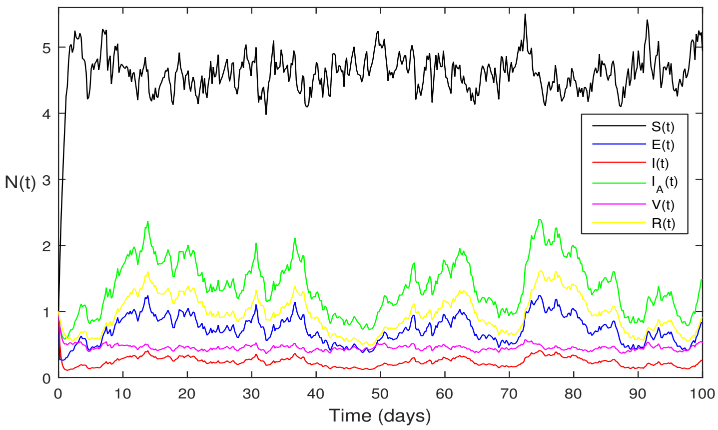


**Figure 4.** Stochastic system Eqs. 2, with $\Lambda = 6, \beta = 2, \beta_A = 1.5, \mu = 1, \mu_1 = 0.9, \phi_1 = 0.4958, \phi_2 = 0.6110, \kappa = 3.871, r = 0.8, \omega_1 = 0.1, \psi = 0.0233, \phi = 0.7$ where $\bar{\mathscr{R}}_0 > 1$.

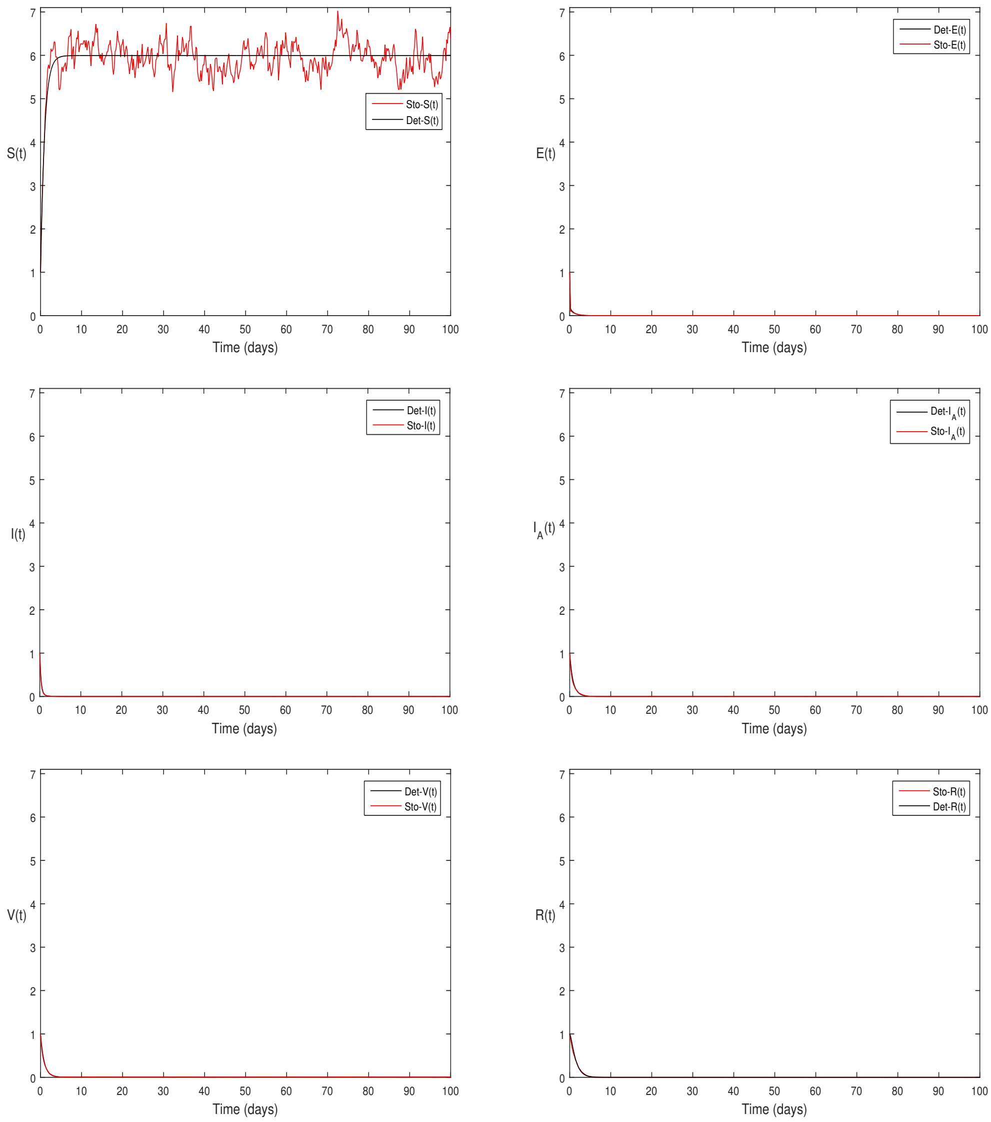


**Figure 5.** Comparison of both the solutions given in Eqs. (1) and Eqs. (2) of each class, for the parameter values $\Lambda = 6, \beta = 1, \beta_A = 1, \mu = 1, \mu_1 = 0.9, \phi_1 = 0.4958, \phi_2 = 0.6110, \kappa = 3.871, r = 0.8, \omega_1 = 0.001, \psi = 0.0233, \phi = 0.7$ where $\bar{\mathscr{R}}_0 < 1$ and $\mathscr{R}_0 < 1$.

 doi:10.20944/preprints202307.1476.v1



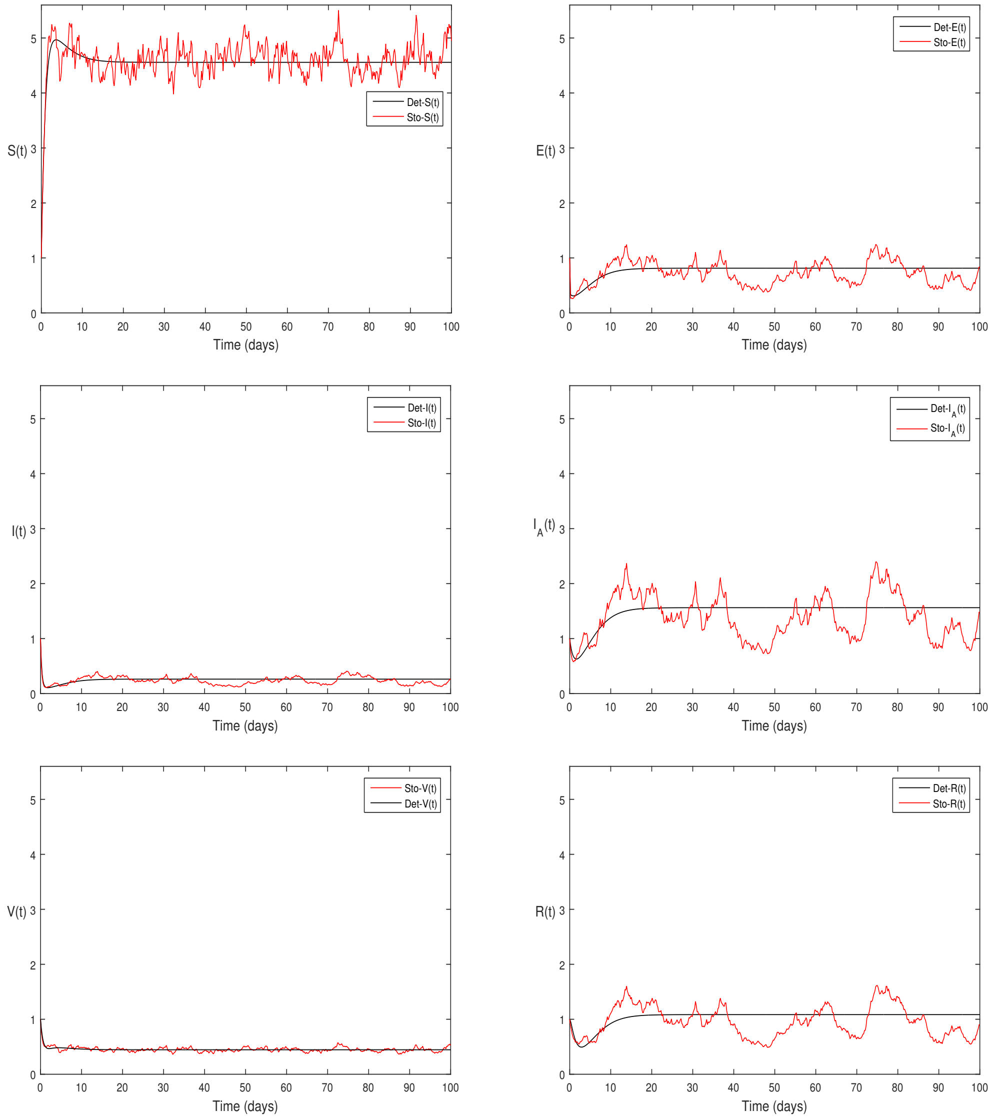


**Figure 6.** Comparison of both the solutions given in Eqs. (1) and Eqs. (2) of each class, for the parameter values $\Lambda = 6, \beta = 2, \beta_A = 1.5, \mu = 1, \mu_1 = 0.9, \phi_1 = 0.4958, \phi_2 = 0.6110, \kappa = 3.871, r = 0.8, \omega_1 = 0.1, \psi = 0.0233, \phi = 0.7$ where $\bar{\mathscr{R}}_0 > 1$ and $\mathscr{R}_0 > 1$.

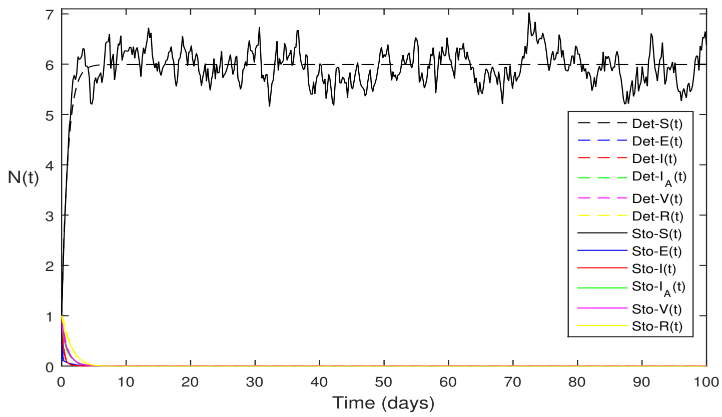


**Figure 7.** Comparison of model Eqs. 1 and model Eqs. 2 solutions taking $\Lambda = 6, \beta = 1, \beta_A = 1, \mu = 1, \mu_1 = 0.9, \phi_1 = 0.4958, \phi_2 = 0.6110, \kappa = 3.871, r = 0.8, \omega_1 = 0.001, \psi = 0.0233, \phi = 0.7$ where $\bar{\mathscr{R}}_0 < 1$ and $\mathscr{R}_0 < 1$.

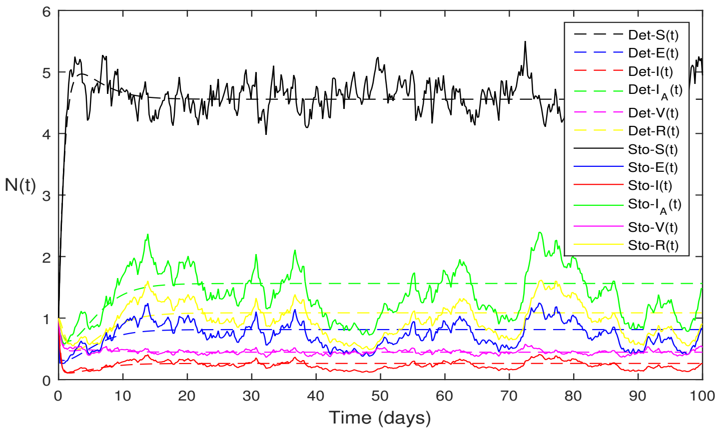


**Figure 8.** Comparison of model Eqs. 1 and model Eqs. 2 solutions taking $\Lambda = 6, \beta = 2, \beta_A = 1.5, \mu = 1, \mu_1 = 0.9, \phi_1 = 0.4958, \phi_2 = 0.6110, \kappa = 3.871, r = 0.8, \omega_1 = 0.1, \psi = 0.0233, \phi = 0.7$ where $\bar{\mathscr{R}}_0 > 1$ and $\mathscr{R}_0 > 1$.

## 6. Conclusions

The use of mathematical modeling combined with numerical analysis using spectral techniques has been shown to be a highly effective approach for gaining deeper insights into the transmission dynamics of diseases. This research introduces a new epidemic model that is analyzed rigorously mathematically to investigate the transmission dynamics of the COVID-19 pandemic, taking into account the impact of vaccination. The crucial measure of disease spread, known basic reproduction number, is found using the next-generation method. Stability of the disease-free equilibrium is proven to be asymptotically stable when the basic reproduction number becomes ($\mathscr{R}_0 < 1$). On the other hand, the stable endemic equilibrium is established when $\mathscr{R}_0$ is greater than 1. To incorporate the effects of vaccination, a vaccination strategy is incorporated into the model. After conducting a various analysis, the proposed models are solved numerically using a highly efficient spectral approach called the high order spectral scheme, which utilizes Legendre collocation nodes. Finally, with the estimated parameter values, the model is simulated to assess the impact of non-pharmaceutical mediation and the effectiveness of vaccination on the transmission dynamics and also to control of the proposed pandemic. In conclusion, the results indicate that by increasing the low transmission rate through preventive calculated like social distancing and following strict SOPs, along with achieving herd immunity through a highly effective vaccine, the pandemic can be effectively curtailed.

**Funding:** Project number (RSPD2023R576), King Saud University, Riyadh, Saudi Arabia.

**Acknowledgments:** Researchers Supporting Project number (RSPD2023R576), King Saud University, Riyadh, Saudi Arabia.

**Conflicts of Interest:** The authors declare no conflict of interest.

## References

1. Ullah, S., Khan, M. A., Farooq, M., and Gul, T. (2019). Modeling and analysis of tuberculosis (TB) in Khyber Pakhtunkhwa, Pakistan. Mathematics and Computers in Simulation, 165, 181-199.
2. Adams, J., MacKenzie, M. J., Amegah, A. K., Ezeh, A., Gadanya, M. A., Omigbodun, A., ... and Silverman, M. (2021). The conundrum of low COVID-19 mortality burden in sub-Saharan Africa: myth or reality. Global Health: Science and Practice, 9(3), 433-443.
3. Mhlanga, A. (2019). Dynamical analysis and control strategies in modelling Ebola virus disease. Advances in Difference Equations, 2019, 1-27.

 doi:10.20944/preprints202307.1476.v1




4. Bhavya, B. M., Doddamani, S. H., and Shubhashree, M. N. (2022). An Overview on Ayurvedic Remedies in Overcoming Communicable Illnesses and Its Contemporary Relevance WSR COVID-19. Rivista Medicine, 2022(1), 149-152.
5. Koca, I. (2018). Analysis of rubella disease model with non-local and non-singular fractional derivatives. An International Journal of Optimization and Control: Theories and Applications (IJOCTA), 8(1), 17-25.
6. Upadhyay, R. K., and Roy, P. (2014). Spread of a disease and its effect on population dynamics in an eco-epidemiological system. Communications in Nonlinear Science and Numerical Simulation, 19(12), 4170-4184.
7. Cai, L. M., Li, Z., and Song, X. (2018). Global analysis of an epidemic model with vaccination. Journal of Applied Mathematics and Computing, 57, 605-628.
8. Li, X. P., Gul, N., Khan, M. A., Bilal, R., Ali, A., Alshahrani, M. Y., ... and Islam, S. (2021). A new Hepatitis B model in light of asymptomatic carriers and vaccination study through Atangana-Baleanu derivative. Results in Physics, 29, 104603.
9. Sulayman, F., Abdullah, F. A., and Mohd, M. H. (2021). An SVEIRE model of tuberculosis to assess the effect of an imperfect vaccine and other exogenous factors. Mathematics, 9(4), 327.
10. Khan, Muhammad Altaf, et al. Global stability and vaccination of an SEIVR epidemic model with saturated incidence rate. *International Journal of Biomathematics* 9.05 (2016): 1650068.
11. Gul, Naseeb, et al. "Transmission dynamic of stochastic hepatitis C model by spectral collocation method." Computer Methods in Biomechanics and Biomedical Engineering 25.5 (2022): 578-592.
12. Ali, Asad, et al. "On dynamics of stochastic avian influenza model with asymptomatic carrier using spectral method." Mathematical Methods in the Applied Sciences (2022).
13. Khan, Sami Ullah and Ali, Ishtiaq. Application of Legendre spectral-collocation method to delay differential and stochastic delay differential equation, AIP Advances, 8, 3,035301, 2018.
14. Khan, Sami Ullah and Ali, Mushtaq and Ali, Ishtiaq. A spectral collocation method for stochastic Volterra integro-differential equations and its error analysis, journal Advances in Difference Equations, Springer, 1, 161, 2019.
15. Khan, Sami Ullah and Ali, Ishtiaq. Numerical analysis of stochastic SIR model by Legendre spectral collocation method, Advances in Mechanical Engineering, SAGE Publications Sage UK: London, England, 11, 7, 2019.
16. Ali, Ishtiaq, and Sami Ullah Khan. Analysis of stochastic delayed SIRS model with exponential birth and saturated incidence rate. Chaos, Solitons and Fractals 138 (2020): 110008.
17. Khan, Sami Ullah and Ali, Ishtiaq. Convergence and error analysis of a spectral collo- cation method for solving system of nonlinear Fredholm integral equations of second kind, Computational and Applied Mathematics Springer, 38, 3, 125, 2019.
18. Khan, Sami Ullah, and Ishtiaq Ali. Applications of Legendre spectral collocation method for solving system of time delay differential equations. Advances in Mechan- ical Engineering 12.6 (2020): 1687814020922113.
19. Yi Song, Anqi Miao, Tongqian Zhang1, Xinzeng Wang, and Jianxin Liu, Extinction and persistence of a stochastic SIRS epidemic model with saturated incidence rate and transfer from infectious to susceptible, *Song et al. Advances in Difference Eqnarrays* (2018) 2018: 293.